

## Asymptotic behavior of equilibrium pair correlations in a dense electron gas

C. Deutsch, Y. Furutani, and M. M. Gombert

*Laboratoire de Physique des Plasmas, Université Paris XI, F-91405 Orsay, France*

(Received 22 December 1975)

The nodal expansion of the potential of average force is worked out systematically by iterating all the nonconvolution compact graphs from the order at which they appear first to infinity. For this purpose, we perform an exhaustive study of the asymptotic behavior of the bridge (without articulation points) graphs, and show that they decrease as  $\beta e^{-\alpha r}/r$ , with  $\alpha > 1$  and  $r$  in units of the Debye length  $\lambda_D$ . We demonstrate that the asymptotic  $w_2(r)$  expansion is obtained from the resummation of the longest convolution chains [ $l \geq 2(n-1)$ ] with  $n-1$  two-bubbles and  $0 \leq c \leq n$  Debye lines, which allow for a systematic improvement of the usual hypernetted-chain (HNC) approximation with the replacement of one, two, or more two-bubbles by bridge graphs. Substantial simplification of the final expression is achieved with the aid of the  $n$ -bubble sum which decreases asymptotically faster than the Debye line. The onset of short-range order is shown to arise at the critical value  $\Lambda_c = 4.247$  of the plasma parameter  $\Lambda = e^2/k_B T \lambda_D$  in excellent agreement with the Del Rio-DeWitt calculations.

### I. INTRODUCTION

The optical diagnostics of hot and dense plasmas considered in the laser fusion program has recently prompted the need for an accurate knowledge of the asymptotic behavior of the pair-correlation function  $g_2(r)$  of the classical one-component and three-dimensional Coulomb gas. Actually, in such plasmas, the strongly degenerate electrons provide the negative background neutralizing the positive and classical ionic charges. For instance, the asymptotic values of  $g_2(r)$  for the ion-ion correlation function are needed in the calculation of the electric microfield experienced by a partially stripped heavy ion, Ar XVIII for instance.<sup>1</sup> The corresponding hydrogenic transitions in the uv domain may then be considered as a spectroscopic tool for the determination of the ion number density.

Recently, many authors<sup>2-4</sup> have devoted themselves to the study of the structure of the expansion, with respect to the plasma parameter  $\Lambda = e^2/k_B T \lambda_D$  ( $\lambda_D^2 = k_B T / 4\pi\rho e^2$  with  $\rho = N_i/V$ ), of the potential of average force  $w_2(r)$  for the one-component Coulomb gas in two<sup>4</sup> and three dimensions<sup>2,3</sup> defined by

$$g_2(r) = e^{\beta w_2(r)}, \quad \beta = (k_B T)^{-1}, \quad (1.1)$$

with  $r$  in units of  $\lambda_D$ . It is already known<sup>2-5</sup> that the longest convolution chains built from  $c (= 0, \dots, n)$  Debye chains and  $n-1$  simple two-bubbles (two Debye chains curved together) provide the most important contribution to the asymptotic behavior of  $g_2(r)$  as far as the nonconvolution graphs of order  $n$  in  $\Lambda$  are considered. Also, several authors<sup>6</sup> have been able to reproduce the Monte Carlo data<sup>7,8</sup> for  $g_2(r)$  with the aid of the hypernetted-chain (HNC) equation with an amazing

accuracy for nearly all values of  $\Lambda$ . These results appear very comforting if one remembers that the sum of the Fourier transforms of the convolution chains with simple two-bubbles for all  $n$  (i.e., the second-order diagrams iterated to infinity) reproduces the content of the HNC equation.<sup>2</sup> More precisely, the HNC numerical procedure is based upon the set of relations

$$w_2(r) = -e^{-r}/r + S(r), \quad (1.2)$$

$$g_2(r) - 1 = T(r) + S(r), \quad (1.3)$$

$$T(r) = G(r) - e^{-r}/r, \quad (1.4)$$

$$S(k) = \frac{k^2 G(k)/(k^2 + 1)}{1 + 1/k^2 - G(k)/\Lambda} - G(k) \quad (1.5)$$

solved by iteration<sup>6</sup> with the initial guess  $S(r) = 0$ .  $S(k)$  denotes the Fourier transform of  $S(r)$ . In this approach the nodal function  $S(r)$  is only derived numerically with the hope that the second-order form (1.5) provides its dominant contribution in the asymptotic range. However, if one wishes to improve the agreement between HNC and the recent Monte Carlo results,<sup>8</sup> one has to work out the complete  $\Lambda$  expansion of  $S(k)$  and take also into account the nonconvolution (bridge) diagrams.

It has been conjectured recently,<sup>6(c)</sup> from a comparison between the new Monte Carlo data for  $g_2(r)$  and the results of HNC for  $\Lambda$  values up to 7000, that the nonconvolution contribution should behave as  $A r^{-1}$  when  $r \rightarrow \infty$ . If this result could be trusted, it would lead one to suspect that the longest convolution chains do not provide the dominant contribution to  $\lim_{r \rightarrow \infty} g_2(r)$ . Obviously, this crucial point deserves a deeper study. Therefore, we pay considerable attention to the asymptotic behavior of the bridge (without articulation point) diagrams,

and we find that the given conjecture is not true. Our analysis is based upon the Mayer-Salpeter<sup>9</sup> expansion of  $w_2(r)$  recently used in two-dimensional cases.<sup>4</sup>

In order to handle easily the asymptotic behavior of high-order graphs ( $n > 3$ ) without spurious difficulties associated with the short-range behavior, we replace, whenever necessary, the classical Coulomb interaction  $r^{-1}$  with an effective one, taking into account the diffraction corrections<sup>11</sup> ( $h \neq 0$ ), i.e.,  $r^{-1}(1 - e^{-Cr})$  with  $C \sim$  (thermal de Broglie wavelength)<sup>-1</sup>. This simple generalization allows us to avoid the introduction from the beginning of the sophisticated resummation<sup>3</sup> of the Meeron graphs, and also to handle finite diagrams to all order  $n$  in  $\Lambda$ . However, the complete  $\Lambda$  expansion for  $w_2(r)$  will be simplified through resummations of topologically equivalent diagrams with the replacement of a Debye line by the sum of  $n$ -bubble ( $l = n, k = 0$ ) diagrams, i.e., an Iwata-Meeron line. The first order in  $\Lambda$ , i.e., the Debye chain including the long-range resummation of the effective interaction, is

$$w_2^1(r) = \frac{-e^2}{r[1 - 4/(c^2\lambda_D^2)]^{1/2}} (e^{-\alpha_1 r} - e^{-\alpha_2 r}), \quad c\lambda_D \geq 2 \quad (1.6)$$

with

$$\alpha_{1,2} = \frac{c}{\sqrt{2}} \left[ 1 \mp \left( 1 - \frac{4}{c^2\lambda_D^2} \right)^{1/2} \right]^{1/2}$$

and

$$\lim_{r \rightarrow \infty} w_2^1(r) = -\frac{e^2}{r} e^{-r}.$$

For the sake of simplicity we shall limit ourselves to the quasiclassical limit with  $\alpha_2 \gg \alpha_1 \sim 1$  and  $w_2^1(r) \sim -e^2 r^{-1} e^{-r}$ .

The paper is organized as follows: In Sec. II, we review briefly the nodal expansion and give a prescription for the determination of the bridge graphs. Section III is devoted to a thorough study of the asymptotic behavior of the fourth-order bridge graphs and the characteristic  $Ae^{-Br}/r$ ,  $B > 1$ , behavior is established. This result is extended to all orders in Sec. IV with the aid of an argument due to Uhlenbeck. Section V outlines the short-range resummation procedure for the sum of  $n$ -bubble diagrams. The nodal expansion of  $w_2(r)$  is detailed in Sec. VI where a generalization of Eq. (1.5) based upon the bridge diagram is presented. The onset of short-range order is also determined.

## II. CONSTRUCTION OF BRIDGE DIAGRAMS

The well-known Salpeter<sup>9,10</sup> version of the Mayer theory for the equilibrium properties of a one-com-

ponent Coulomb gas leads to a  $\Lambda$  expansion of  $w_2(r)$  already discussed at length in Ref. 4. Therefore we may skip over the corresponding fundamentals providing one remembers that a given nodal graph ( $l, k$ ) is a connected structure made of  $l$  Debye chains [Eq. (1.6)] and  $k$  nodal (field) points, where at least three Debye lines merge and fulfill the condition  $l - k = n$ ,  $n$  being the order of the  $\Lambda$  expansion. The root points 1 and 2 correspond to the reference ones arising from  $g_2(|\vec{r}_1 - \vec{r}_2|)$ . It is a well-known fact that the first nonconvolution graphs appear with the third order.<sup>3,4</sup> It must also be emphasized that we focus our attention on the nodal 12 irreducible graphs<sup>12</sup> because the 12 reducible graphs of order  $n$  are easily calculated in the configuration space as products<sup>21</sup>: (Debye chains)  $\times$  (convolution chains) or (Debye chains)  $\times$  [12 irreducible bridge ( $n - 1$ ) nodal]. "Bridge ( $n$ )" denotes a bridge graph of order  $n$ . The third- and fourth-order nodal bridge diagrams are displayed in Fig. 1.

The 12 reducible graphs given as the products (Debye chains)  $\times$  [convolution chains ( $n - 1$ )] are not included in the  $\Lambda$  expansion (nodal) of  $w_2(r)$ . However, they still belong to the  $\Lambda$  expansion of  $g_2(r)$ . Moreover they are also used to build up convolution chains of importance in the asymptotic range of  $w_2(r)$ . Some of these are given in Fig. 2. They are easily evaluated from the ( $n - 1$ )-convolution chains, so we did not need to pay much attention<sup>12</sup> to their calculation, and we may concentrate our

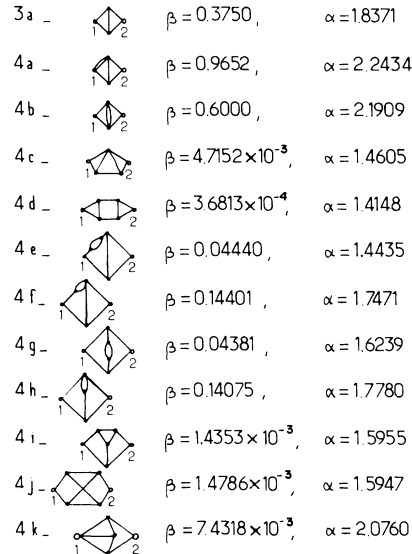


FIG. 1. Third- and fourth-order nodal bridge graphs. The first one is third order while the remaining ones are fourth order. The asymptotic decrease  $C\beta e^{-\alpha r}/r$ , with  $C = (-1)^l (4\pi)^n / (2\pi)^{3-n-1}$ , is parametrized by  $\beta$  and  $\alpha > 1$ .

efforts on the 12 irreducible nodal bridge diagrams.

First, we have to construct these graphs to all orders with the simple recipe: Join two points (root or nodal), a line and a point or two lines in a 12 irreducible bridge ( $n-1$ ), so that they are all generated from the single bridge (3). The counting problem is a much more difficult task, because the above process could lead to several topologically (numerically) equivalent graphs. Hopefully, it does not prevent us from getting the relative number of bridge diagrams and convolution chains. More precisely, in view of controlling order by order the asymptotic behavior of the expansion, we need to know both the number and the asymptotic behavior of each  $n$ -order graph. A Herculean task! However, we shall see that it is possible to predict the asymptotic behavior of each class of graphs: convolution, mixed, bridge. This result, combined with the possibility of comparing the relative number of graphs with given  $k$ , gives access to an asymptotic behavior uniform with respect to  $n$ . The Fourier-transform convolution methods make it clear that, at infinity, the graphs containing at least one articulation point decrease slower than the  $p$ -bubbles ( $l=p$ ,  $k=0$ ) or the bridge graphs building them. Moreover, the dominant graph at infinity with given  $l \geq 2(n-1)$  and  $k$  is the longest convolution chain made of  $n-1$  two-bubbles and  $c(=0, 1, \dots, n)$  Debye lines in between. On the other hand, it may be easily shown that the graphs with  $n \leq l \leq 2(n-1)$  mostly contribute to the  $r=0$  range, while their asymptotic behavior is monitored by the  $p$ -bubbles with  $p \geq 2$ . Their topological structure is already present at order  $n-1$ , and differs only from the corresponding graphs by one more line between any points, so their asymptotic behavior gets faster. As a provisional conclusion, we may state that the Fourier-transform convolution methods allow for an order-by-order determination of the dominant asymptotic contribution provided one knows how to handle the nonconvolution contributions arising from the 12 irreducible bridge graphs.

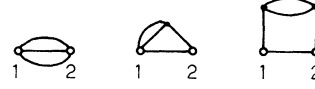


FIG. 2. Third-order 12 reducible diagrams arising in the  $g_2(r)$   $\Lambda$  expansion, and contributing to the chains building up the  $w_2(r)$  asymptotic expansion.

### III. FOURTH-ORDER BRIDGE DIAGRAMS

The purpose of the present section is to determine the asymptotic behavior of the third- and fourth-order bridge graphs displayed in Fig. 1. This study is a necessary prerequisite for further examination of the  $w_2(r)$   $\Lambda$  expansion. Our approach is based on a clever treatment due to Mitchell and Ninham for the third-order graph (3a) that we follow quite closely and extend, whenever necessary, to the fourth-order graphs with the aid of new relations made explicit in Appendix A. These methods differ in many respects from the standard Fourier-transform convolution methods used for the convolution graphs.<sup>2-5</sup> This explains the rather technical character of this section, although we try to remain as concise as possible without being obscure.

In order to lay down our technical basis we analyze in some detail the asymptotic behavior of the simplest nodal 12 irreducible bridge diagram (3a) appearing with the third order. Labeling the nodal points in an obvious way, the corresponding Mayer-Salpeter integral is ( $r = |\vec{r}_1 - \vec{r}_2|$ ,  $r_{ij} = |\vec{r}_j - \vec{r}_i|$  with  $i, j \neq 1, 2$ )

$$w_3^a(r) = (-\beta e^2)^5 \rho^2 \int \int d\vec{r}_3 d\vec{r}_4 \frac{e^{-r_{31}}}{r_{31}} \frac{e^{-r_{41}}}{r_{41}} \times \frac{e^{-r_{43}}}{r_{43}} \frac{e^{-r_{32}}}{r_{32}} \frac{e^{-r_{42}}}{r_{42}}, \quad (3.1)$$

with  $r$  and  $r_{ij}$  in units of  $\lambda_D$ . Let us introduce

$$\frac{e^{-r_{ij}}}{r_{ij}} = (2\pi^2)^{-1} \int \frac{d\vec{k} e^{i\vec{k} \cdot \vec{r}_{ij}}}{1+k^2}, \quad (3.2)$$

whence

$$w_3^a(r) = \frac{(-\beta e^2)^5 \rho^2}{(2\pi^2)^5} \int \int d\vec{r}_3 d\vec{r}_4 \int \prod_{i=1}^5 \frac{d\vec{k}_i}{(1+k_i^2)} \exp[-i(\vec{k}_1 + \vec{k}_2) \cdot \vec{r}_1 + i(\vec{k}_3 + \vec{k}_4) \cdot \vec{r}_2 + i(\vec{k}_1 - \vec{k}_3 - \vec{k}_5) \cdot \vec{r}_3 + i(\vec{k}_2 - \vec{k}_4 - \vec{k}_5) \cdot \vec{r}_4] \\ = \frac{(-\beta e^2)^5 \rho^2}{(2\pi^2)^5} \int d\vec{k}_1 d\vec{k}_2 d\vec{k}_3 \frac{e^{i(\vec{k}_1 + \vec{k}_2) \cdot \vec{r}}}{(1+k_1^2)(1+k_2^2)(1+k_3^2)[1+(\vec{k}_1 + \vec{k}_2 - \vec{k}_3)^2][1+(\vec{k}_1 - \vec{k}_3)^2]}. \quad (3.3)$$

The last line obtained with  $\vec{k}_1 + \vec{k}_2 = \vec{k}_3 + \vec{k}_4$  makes it convenient to introduce the Fourier transform

$$w_3^a(k) = -\frac{\Lambda^3 (4\pi)^3}{(2\pi^6)} \int d\vec{P} d\vec{Q} \frac{1}{(1+P^2)[1+(\vec{P} + \vec{k})^2][1+(\vec{P} - \vec{Q})^2][1+(\vec{Q} + \vec{k})^2](1+Q^2)}, \quad (3.4)$$

where  $\vec{Q} = -\vec{k}_1 - \vec{k}_3 - \vec{k}_5$  and  $\vec{P} = -\vec{k}_1$ . Now, the relation (see Appendix A)

$$I_1 \equiv \int \frac{d\vec{Q}}{(\mathcal{Q}^2 + \alpha^2)[(\vec{Q} + \vec{k})^2 + \beta^2][(\vec{Q} + \vec{P})^2 + \gamma^2]} = \pi^2 \int_0^1 \frac{dx}{\delta[(\vec{P} - x\vec{k})^2 + (\gamma + \delta)^2]},$$

$$\delta^2 = x(1-x)k^2 + x\beta^2 + (1-x)\alpha^2 \quad (3.5)$$

is useful. Using this twice with  $\alpha = \beta = 1$ , we have

$$w_3^a(k) = -\pi\Lambda^3 \int_0^1 \frac{dx}{\delta} \int_0^1 \frac{dy}{\delta'} \frac{1}{k^2(x-y)^2 + (1+\delta+\delta')^2}, \quad (3.6)$$

with  $\delta^2 = x(1-x)k^2 + 1$  and  $\delta'^2 = y(1-y)k^2 + 1$ . Equation (3.6) is the Mitchell-Ninham result.<sup>5</sup> It is a very convenient form to work out the asymptotic expansion of  $w_3^a(k)$ , which can be obtained through its small- $k$  limit,

$$\begin{aligned} w_3^a(k) &= -\pi\Lambda^3 \int_0^1 dx \int_0^1 dy \frac{[1 - x(1-x)k^2/2 - y(1-y)k^2/2]}{k^2(x-y)^2 + 9[1 + x(1-x)k^2/6 + y(1-y)k^2/6]^2} \\ &= -\frac{\pi\Lambda^3}{9} \left(1 - \frac{8k^2}{27}\right) = -\frac{3\pi\Lambda^3}{8} \frac{1}{k^2 + \frac{27}{8}}, \quad k^2 \ll 1 \end{aligned} \quad (3.7)$$

which shows the characteristic faster-than-Debye decrease at infinity,

$$w_3^a(r) \sim -\frac{0.375\Lambda^3 e^{-1.8371r}}{4r}, \quad \text{as } r \rightarrow \infty. \quad (3.8)$$

These last relations together with Eq. (3.5) exhibit the main features of our techniques applied to the fourth-order graphs. First, we eliminate angular averages as much as possible with the aid of Eq. (3.5) and its extended version considered in Appendix A. Second, we look for  $\lim_{k \rightarrow 0} w_3(k)$  in the form  $C(A - Bk^2)$ , corresponding to the asymptotic decrease  $C\beta e^{-\alpha r}/r$  with  $\beta = A^2/B$  and  $\alpha = (A/B)^{1/2}$ . As will be shown below, one recovers again  $\alpha > 1$ , this making clear that the 12 irreducible bridge graphs decrease faster than  $e^{-r}/r$  for  $r \rightarrow \infty$ . With no further specification in the sequel,  $\delta$  is given by the  $\delta^2 = x(1-x)k^2 + 1$  definition.

At this point a certain amount of warning has to be injected. The present analysis could be appreciated as truly quantitative only when the full asymptotic expansion  $a - bk^2 + ck^4 - dk^6 + \dots$  is obtained.<sup>13</sup> However, we are mostly interested in demonstrating the  $e^{-\alpha r}/r$  asymptotic decrease with  $\alpha > 1$ , i.e.,  $ab > 0$  and  $b/a < 1$ , so the  $a - bk^2$  approximation appears sufficient for this purpose. In order to convince oneself that Eq. (3.8) provides only an approximate upper bound to the true asymptotic behavior, let us contemplate the Cauchy-Schwartz inequality

$$\begin{aligned} |w_3^a(r_{12})| &\leq \int d\vec{r}_3 \frac{e^{-2r_{13}}}{r_{13}^2} \frac{e^{-2r_{32}}}{r_{32}^2} \int d\vec{u} \frac{e^{-u}}{u} \\ &= \frac{4\pi e^{-2r_{12}}}{r_{12}^3} \quad \text{as } r_{12} \rightarrow \infty, \end{aligned} \quad (3.8')$$

with the convolution product of two two-bubbles

explained in Appendix B. This new upper bound decreases much faster than (3.8). Nevertheless, the  $a - bk^2$  analysis of the fourth-order bridge graphs remains of interest to demonstrate their faster-than-Debye asymptotic decrease. In a future work, we will explain the tedious  $O(k^{2n})$  contributions with  $n \geq 2$ .

We now consider the fourth-order irreducible bridge graphs in order of increasing complexity. The simplest one is

$$w_4^a(r) = \frac{\rho^2(\beta e^2)^6 \pi^2}{(2\pi^2)^5} \frac{\pi^2}{2} \int_0^1 \frac{dx}{\delta} \int d\vec{Q} \frac{\tan^{-1}(Q/2)}{Q} \frac{1}{1 + (\vec{Q} - \vec{k})^2} \times \frac{1}{(\vec{Q} - x\vec{k})^2 + (1 + \delta)^2}. \quad (3.9)$$

Here the following two relations are in order

$$\frac{1}{[1 + (\vec{Q} - \vec{k})^2][(\vec{Q} - x\vec{k})^2 + (1 + \delta)^2]} = \int_0^1 \frac{dy}{[(\vec{Q} - A\vec{k})^2 + B^2]^2}$$

and

$$\tan^{-1}\left(\frac{Q}{2}\right) = \int_0^\infty \frac{dt}{t} e^{-rt} \sin Qt, \quad (3.10)$$

with  $A = 1 - y(1-x)$  and  $B^2 = 1 + [(1+\delta)^2 - 1]y + k^2y(1-y)(1-x)^2$ . We then obtain

$$w_4^a(k) = \pi\Lambda^4 \int_0^1 \frac{dx}{\delta} \int_0^1 \frac{dy}{A B k} \tan^{-1}\left(\frac{A k}{2+B}\right). \quad (3.11)$$

The corresponding asymptotic behavior is given by

$$\begin{aligned} w_4^a(k) &= \pi\Lambda^4(0.19179 - 0.038109k^2), \quad k^2 \ll 1, \\ w_4^a(r) &\sim 0.96522\Lambda^4 e^{-2.2434r}/4r, \quad \text{as } r \rightarrow \infty. \end{aligned} \quad (3.12)$$

The same techniques apply to (4k). Longer graphs are treated in a similar way with repeated use of Eq. (3.5). For instance,  $w_5^a(k)$  reads

$$w_4^c(k) = -\frac{\pi\Lambda^4}{2} \int_0^1 \frac{dx}{\delta} \int_0^1 \frac{dy}{\delta'} \int_0^1 \frac{dz}{\delta''} \frac{1}{(x-z)y^2k^2 + (1+\delta+\delta'')^2}, \quad (3.13)$$

with  $\delta'^2 = 1 + k^2y(1-y)$  and  $\delta''^2 = z(1-z)y^2k^2 + z(1+\delta')^2 + 1-z$ . In the  $k^2 \ll 1$  limit, the above integral is evaluated as

$$w_4^c(k) = -\frac{\pi\Lambda^4}{36} \left(1 - \frac{4.2192}{9}k^2\right), \quad k^2 \ll 1$$

from which follows

$$w_4^c(r) \sim -\frac{1.1901\Lambda^4}{8} \frac{e^{-1.4605r}}{r} \quad \text{as } r \rightarrow \infty. \quad (3.14)$$

The  $I_2$  quadrature (A6) allows us to evaluate  $[\eta^2 = 1 + k^2x(1-x), \eta'^2 = 1 + k^2y(1-y)]$

$$w_4^d(k) = \frac{\pi\Lambda^4}{2} \int_0^1 \frac{dx}{\eta} \int_0^1 \frac{dy}{\eta'} \int_0^1 d\vec{k}_3 \frac{1}{(1+k_3^2)[1+(\vec{k}-\vec{k}_3)^2][(\vec{k}_3-x\vec{k})^2+(1+\eta)^2][(\vec{k}_2-y\vec{k})^2+(1+\eta')^2]}$$

in a straightforward way:

$$w_4^d(k) = \frac{\pi\Lambda^4}{2} \times 3.6813 \times 10^{-4} \frac{1}{(1.4148)^2 + k^2}, \quad k^2 \ll 1 \quad (3.15)$$

giving

$$w_4^d(r) \sim \frac{1}{8}\pi\Lambda^4 \times 3.6813 \times e^{-1.4148r}/r \quad \text{as } r \rightarrow \infty. \quad (3.16)$$

Next, we consider the four graphs (4e), (4f), (4g), and (4h) obtained from (3a) upon replacing one Debye line by a second-order convolution chain. They are easily evaluated in the asymptotic limit with the aid of Eq. (A6), and we do not need to detail their derivation. We are thus left with the compact topologies (4i), (4j), and (4k). As an example, let us consider

$$w_4^j(k) = \frac{(4\pi)^4\Lambda^4}{(2\pi)^6} \int d\vec{k}_1 d\vec{k}_2 d\vec{k}_3 \frac{1}{1+(\vec{k}-\vec{k}_2-\vec{k}_3)^2} \frac{1}{1+(\vec{k}-\vec{k}_1-\vec{k}_2-\vec{k}_3)^2} \frac{1}{1+(\vec{k}-\vec{k}_1-\vec{k}_3)^2} \frac{1}{(1+k_1^2)(1+k_2^2)(1+k_3^2)} \\ \times \frac{1}{1+(\vec{k}_2+\vec{k}_3)^2} \frac{1}{1+(\vec{k}_1+\vec{k}_3)^2}. \quad (3.17)$$

Performing the  $\vec{k}_1$  and  $\vec{k}_2$  quadratures with Eq. (A6), and introducing  $\vec{Q} = \vec{k}_1 + \vec{k}_2$ , one gets

$$w_4^j(k) = \frac{\Lambda^4}{2\pi} \int_0^1 \frac{dx}{\delta} \int_0^1 dy \int_0^1 du \int_0^1 d\vec{Q} \frac{\delta + \delta' + \eta}{\eta\delta'} \frac{1}{(1+Q^2)[1+(\vec{Q}-\vec{k})^2]\{(1-y-u)\vec{Q} - (x-y)\vec{k}\}^2 + (\delta + \delta' + \eta)^2}, \quad (3.18)$$

where  $\delta'^2 = 1 + (Q-k)^2y(1-y)$  and  $\eta^2 = 1 + Q^2u(1-u)$ . The usual  $k^2 \ll 1$  limit is given by the involved expression

$$w_4^j(k) \simeq 2\Lambda^4(1.1477 \times 10^{-2} - 4.5131 \times 10^{-3}k^2), \quad k^2 \ll 1. \quad (3.19)$$

The corresponding triple integral has been worked out through a Monte Carlo calculation. Analogous manipulations are used for the graphs (4i) and (4k). All the fourth-order results are summarized with appropriate  $\alpha$  and  $\beta$  values given in Fig. 1.

The simpler 12 reducible graph arising from these compact structures is obtained with the product

$-e^{-r}/r \times (3a) = 0.375 \times e^{-2.871r}/4r^2$ . We have thus completed the proof that all fourth-order bridge graphs decrease faster than the Debye potential at infinity. Analogous results may be obtained in a much easier way for the 12 reducible graphs which are products of Debye lines and convolution chains.<sup>5</sup> As an example, the third-order 12 reducible contribution (three-bubble excepted) depicted in Fig. 2 may be written as

$$-\frac{1}{8} \left( \frac{\ln 3}{2+k^2/6} - \frac{2}{9+19k^2/12} + \frac{2}{9+k^2/9} - \frac{2}{3+k^2/9} \right) \\ + 2 \left( \frac{\ln 3}{2+k^2/6} + \frac{2}{9+k^2/9} \right), \quad k^2 \ll 1. \quad (3.20)$$



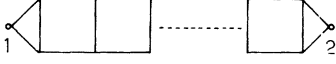


FIG. 5. Longest bridge graph with  $I = 2$  (horizontal ladder).

(4.1) and analogous expressions for compact graphs obtained in Appendix B provide the upper bound

$$|C(m_2, k' \leq k)| \leq r^m e^{-I'r} / (4\pi)^{k'}, \quad r \rightarrow \infty. \quad (4.3)$$

The upper bound (4.1) has been introduced into (4.3) through noting that the line connection degree of a bridge graph is equal to its point connection degree, i.e.,  $I = I'$ . The same property holds also for the associated fictitious graph. As a consequence, the right-hand side of Eq. (4.2) becomes

$$(4\pi)^{-k} \sum_{m=1}^{I-2} \frac{1.38^m}{(4\pi)^{k\tau}} r^m e^{-I'r}. \quad (4.4)$$

This result combined with the inequality (4.1) finally yields

$$|B(l, k)| < \frac{l(1.38)^{l-2}}{(4\pi)^k} r^m e^{-I'r}, \quad r \rightarrow \infty \quad (4.5)$$

with  $m \geq 2$  for all  $n$  and  $l/(4\pi)^k \ll 1$  when  $n \rightarrow \infty$ . At the moment, we restrict ourselves to single-bonded graphs, so that  $k \sim 2n$  and  $l \sim 3n$  when  $n \rightarrow \infty$ . Looking back at the Cauchy-Schwarz upper bound obtained for  $|w_3^a(r)|$ , one sees that the pinching process leading to (4.2) is actually producing upper bounds to the asymptotic estimates.

Finally, the inequality (4.5) extends to all  $n$  the previous results obtained for  $n = 3$  and  $n = 4$ . Now, we may compare order by order the rapid decaying-at-infinity bridge graphs with the longest convolution chains  $\sim r^{n-2} e^{-r}$  as  $r \rightarrow \infty$ . Although the present proof extends the previous findings to any  $n$ , it complements rather than supplements the calculations of Sec. III which are used to obtain Eq. (4.5). Moreover, another extension of these latter methods is needed to derive accurate estimates for higher-order bridge graphs involved in the asymptotic expansion of  $w_2(r)$  considered in Sec. IV B. A more deductive derivation of these results will be given elsewhere.<sup>12</sup>

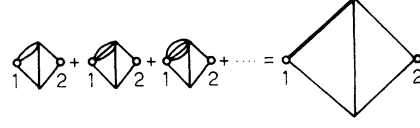


FIG. 6. Resummation to all orders of  $n$ -bubble bonds in a nodal bridge graph.

### B. Bridge graphs with multiple bonds

We could have obtained results similar to the previous ones for the case of double bonds through the introduction of  $4\pi \int_0^\infty dx x^2 (e^{-x}/x)^2 = 4.91$  in Eq. (4.2). However, we must face the general situation of an  $n$ -multiple bond with  $n > 2$  and circumvent the difficulties associated with the nonsummability at the origin of any power of the classical Debye potential. Obviously, we could work with the effective interaction (1.6) fulfilling

$$\int_0^\infty dr r^2 |w_2^1(r)|^n < +\infty, \quad \text{all } n. \quad (4.6)$$

Although this trick is qualitatively and conceptually sufficient to secure a well-defined  $\Lambda$  expansion for  $w_2(r)$ , the increasing absolute value of the estimate (4.6) makes it improper to yield a quantitative determination of the asymptotic behavior of bridge graphs. As a consequence, we have to cope with the familiar resummation to all orders of the most diverging graphs in the  $r \rightarrow 0$  limit, as is depicted in Fig. 6 for the simplest 12 irreducible bridge graph.

This difficulty has already been encountered by many authors,<sup>2-4</sup> and was solved with various degrees of sophistication. To our knowledge, however, there exists no exhaustive study of the  $n$ -bubble sum in  $k$  space together with its asymptotic behavior necessary for the purpose of comparison with the single-bonded bridge graphs considered so far. This shortage explains why we performed elsewhere<sup>16</sup> a comprehensive investigation of the Fourier transform

$$f(k) = \frac{\Lambda}{2\pi^2 k} \int_0^\infty dr r \operatorname{sinc} kr \left[ \exp\left(-\frac{\Lambda e^{-\alpha r}}{r}\right) - 1 + \frac{\Lambda e^{-\alpha r}}{r} \right] \quad (4.7)$$

for the  $n$ -bubble sum  $\sum_{n=2}^\infty \{[-\Lambda w_2^1(r)]^n / n!\}$ . Here, we limit ourselves to stress the main results of interest for the present work. Expression (4.7) may be written as

$$f(k) = \frac{\Lambda^2}{2\pi^2 k} \sum_{n=2}^\infty \frac{1}{\Gamma(n-1)\Gamma(n+1)} \left(\frac{an}{\cos\theta_n}\right)^{n-2} \left\{ \left[ \ln\left(\frac{an}{\cos\theta_n}\right) - \psi(n-1) - \psi(n+1) \right] \sin[(n-2)\theta_n] + \theta_n \cos[(n-2)\theta_n] + \frac{n-2}{2} \cos\theta_n \sin[(n-3)\theta_n] \right\} \quad (4.8)$$

$$\psi(n) = \frac{\Gamma'(n)}{\Gamma(n)},$$

where  $\tan\theta_n = b/an$ ,  $a = \alpha\Lambda$  and  $b = k\Lambda$ , and  $\psi(n)$  is the di-gamma function. As was conjectured previously,<sup>3</sup>  $f(k)$  is a double power series in  $\Lambda$  and  $\ln\Lambda$ , equivalent to Eq. (19) of Ref. 2, as may be seen by setting  $n - ik = (n^2 + k^2)^{1/2} e^{-i\theta_n}$  with  $\tan\theta_n = k/n$  in their result. We are mostly interested in the small- $k$  expression (the subscript  $\alpha = 1$  is deleted hereafter)

$$f(k) = \frac{\Lambda^2}{2\pi^2 k} \left[ \frac{\tan^{-1}(k/2)}{2!} + \sum_{l=0}^{\infty} (-1)^l \frac{l(k\Lambda)^{2l+1}}{(2l+1)!} \sum_{n=3}^{\infty} \frac{(\Lambda n)^{n-2l-3}}{\Gamma(n+1)\Gamma(n-2l-3)} \left( \ln(\Lambda n) + \frac{n-2l-3}{n} - \psi(n+1) - \psi(n-2l-2) \right) \right], \quad (4.9)$$

and its asymptotic expression

$$f(k) = (\Lambda^2/2\pi^2) [A(\Lambda) - B(\Lambda)k^2], \quad k^2 \ll 1 \quad (4.10)$$

where

$$A(\Lambda) = \frac{1}{4} + \Lambda \sum_{n=3}^{\infty} \frac{(\Lambda n)^{n-3}}{\Gamma(n+1)\Gamma(n-2)} \left( \ln(\Lambda n) + \frac{n-3}{n} - \psi(n+1) - \psi(n-2) \right) \quad (4.11)$$

and

$$B(\Lambda) = \frac{1}{6} \left[ \frac{1}{8} - \frac{\Lambda}{54} + \frac{\Lambda^2}{96} + \Lambda^3 \sum_{n=5}^{\infty} \frac{(\Lambda n)^{n-5}}{\Gamma(n+1)\Gamma(n-4)} \left( \ln(\Lambda n) + \frac{n-5}{n} - \psi(n+1) - \psi(n-4) \right) \right]$$

are positive and monotonically decreasing functions of  $\Lambda$ , so that  $f(r)$  displays the Debye-like asymptotic decrease

$$f(r) \sim \Lambda^2 \beta e^{-\alpha r} / r \quad \text{for } r \rightarrow \infty, \quad \alpha = (A/B)^{1/2}, \quad \beta = A^2/B. \quad (4.12)$$

Extensive numerical analyses of  $A(\Lambda)$  and  $B(\Lambda)$  have been carried out.<sup>16</sup> We give in Table I their values for  $0.1 \leq \Lambda \leq 10$  in order to show the reader the slowly decreasing behavior of  $f(r)$  at infinity, which is so important in extending the previous results to multiple-bonded bridge graphs.  $B(\Lambda)$  is about one order of magnitude smaller than  $A(\Lambda)$ . Then  $\beta > 1$  ensures a faster-than-Debye asymptotic decrease with respect to  $r$ . This point is funda-

TABLE I. Values of  $A(\Lambda)$  and  $B(\Lambda)$  for Eq. (4.11).

$\Lambda$	$A(\Lambda)$	$B(\Lambda)$
0.1	0.213 97	0.020 539
0.2	0.195 59	0.020 268
0.3	0.182 26	0.020 015
0.4	0.171 72	0.019 777
0.5	0.162 98	0.019 551
1.0	0.135 56	0.018 570
2.0	0.102 92	0.017 070
3.0	0.085 724	0.015 925
4.0	0.074 267	0.015 007
5.0	0.065 929	0.014 096
6.0	0.059 520	0.013 575
7.0	0.054 403	0.012 918
8.0	0.050 201	0.012 488
9.0	0.046 678	0.012 031
10.0	0.043 672	0.011 619

mental in that it will allow us below to neglect most of the multiple-bonded bridge graphs when compared to the single-bonded ones. However, our main concern is to extend the estimate (4.5) to a bridge graph with a  $f(r)$  bond, as is shown in Fig. 6. Again the previous lines of reasoning apply in the present situation, provided one replaces the Debye quadrature for short bonds with

$$I \equiv \int_0^{r_0} dr r^2 \left[ \exp\left(-\frac{\Lambda e^{-r}}{r}\right) - 1 + \frac{\Lambda e^{-r}}{r} \right], \quad (4.13)$$

whose value is given numerically in Table II. As before  $r_0$  is defined by  $\exp(\Lambda e^{-r_0}/r_0) - 1 + \Lambda e^{-r_0}/r_0 = r_0$ . It then remains to note the faster-than-Debye decrease at infinity of all the bridge graphs with the exception of the horizontal ladder single-connected graphs (longest bridge graphs) decaying faster than the corresponding chain of  $n-1$  two-bubbles.

TABLE II. Short bond for multiple-bonded bridge graphs.

$\Lambda$	$r_0$	$I$
0.1	0.23	$6.22 \times 10^{-4}$
0.2	0.31	$2.75 \times 10^{-3}$
0.3	0.366	$6.24 \times 10^{-3}$
0.4	0.411	$1.13 \times 10^{-2}$
0.5	0.449	$1.77 \times 10^{-2}$
0.6	0.482	$2.50 \times 10^{-2}$
0.7	0.511	$3.77 \times 10^{-2}$
0.8	0.537	$4.37 \times 10^{-2}$
0.9	0.561	$5.40 \times 10^{-2}$
1.0	0.583	$6.54 \times 10^{-2}$

## V. ASYMPTOTIC BEHAVIOR OF THE PAIR-CORRELATION FUNCTION

### A. Asymptotic structure of the $w_2(r)$ nodal expansion to all orders in $\Lambda$

The above results enable us to make quantitative the program outlined in Sec. III for a systematic comparison of the different classes of graphs in the asymptotic range. For the sake of clarity, we display in Figs. 7 and 8 all the numerically distinct third- and fourth-order nodal graphs. The corresponding graphs (not simple according to Ref. 9) appearing in the  $\Lambda$  expansion of  $g_2(r)$  are obtained by factorizing the nodal graphs of order  $n-1$  with a Debye line joining the root points. The graphs are given following their increasing  $l$  and  $k$  values to visualize easily the basic processes generating all the nodal graphs up to an arbitrary order  $n$ . The first striking feature displayed by this comparison is that no new topological structure for  $k < 2(n-2)$  appear, within the convolution subclass. The new graphs are only low-order graphs decorated with one more ( $ij$ ) Debye bond. It then appears feasible to resum them from the order where they appear first to infinity through the  $n$ -bubble sum previously investigated. The resummation of these compact structures could open the way to an accurate determination of  $\lim_{r \rightarrow 0} w_2(r)$ , which will be reserved for a future work.

On the other hand, new convolution structures appear with  $l \geq 2(n-1)$  which get longer and more important in the  $r \rightarrow \infty$  limit. The longest chain  $[3n-2, 2n-2]$  with  $n-1$  two-bubbles and  $n$  Debye lines is the dominant graph in the asymptotic range. However, once the detailed  $w_2(r)$   $\Lambda$  expansion is known, it is no longer *a priori* convincing to restrict  $\lim_{r \rightarrow \infty} w_2(r)$  to this graph iterated to all orders. Actually, the number of bridge graphs

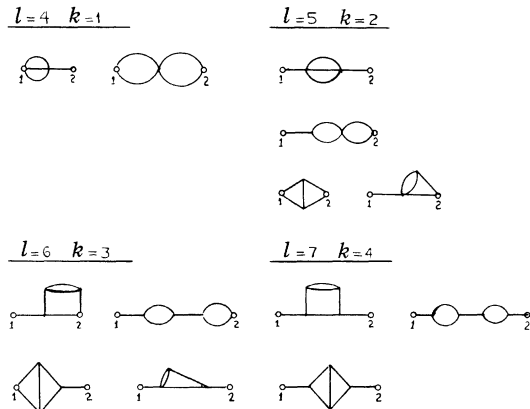


FIG. 7. Numerically distinct nodal third-order graphs given according to their  $[l, k]$  values.

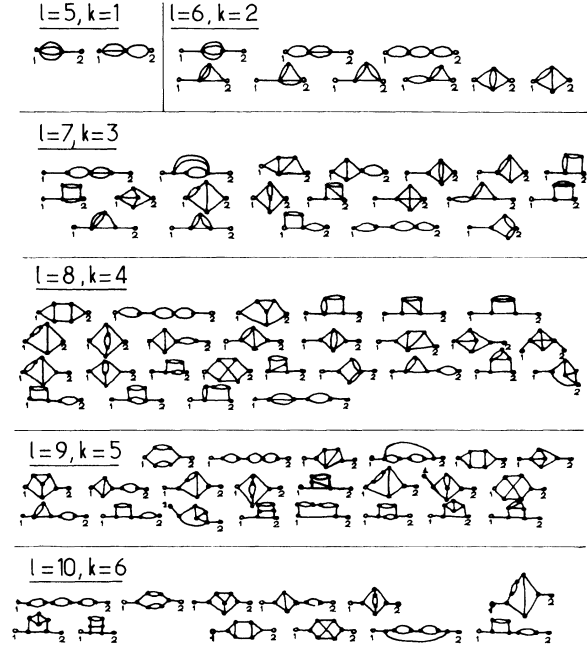


FIG. 8. Numerically distinct nodal fourth-order graphs given according to their  $[l, k]$  values.

and their associated mixed structures (bridges with adjacent convolution chains) increases much more rapidly than the number of convolution chains built from  $n$ -bubbles ( $n \geq 2$ ). Nevertheless, it is still noticeable that the convolution chain built from  $n-1$  two-bubbles and  $0 \leq c \leq n$  Debye lines should provide the dominant asymptotic contribution

$$\begin{aligned} \lim_{r \rightarrow \infty} |C'(l, k)| & \approx \frac{2}{\pi r} \frac{n!}{(n-c)! c!} \int_0^\infty \frac{dp p \sin pr}{(p^2+1)^c} \left( \frac{\tan^{-1}(p/2)}{2p} \right)^{n-1} \\ & \approx \frac{2}{\pi r} \frac{n!}{(n-c)! c! (c-1)!} \frac{r^{c-2} e^{-r}}{2^{2(n-1)+c-1}} \end{aligned} \quad (5.1)$$

[ $C'(l, k)$  is a convolution graph], within each  $(l, k)$  subclass with  $l > 2(n-1)$ . In order to establish on firmer grounds the expected asymptotic preeminence of the longest convolution chains, we need an argument powerful and simple enough to circumvent the very difficult task of evaluating the number of graphs within each class: convolution, bridge, and mixed. The remark which will prove instrumental toward that goal is afforded by observing the way a given topological structure travels through the nodal expansion. A new compact (12 irreducible or 12 reducible bridge) graph without adjacent Debye chains is first translated to order  $n+1$  with the addition of a Debye line between the already existing points (nodal + roots)

with  $(l, k) \rightarrow (l+1, k)$ . It further propagates to the higher subclasses  $(l+2, k+1)$  and  $(l+3, k+2)$  through convolution with one and two Debye lines respectively. It is a process efficient enough to provide all the mixed structures with  $l > 2(n-1)$ , i.e., those competing seriously with the corresponding  $(l, k)$  convolution chains in the asymptotic range. Putting aside the special case of the horizontal ladder immediately compared to the  $(n-1, 0)$  convolution chain, we learned from Sec. IV that any compact graph may be given the asymptotic estimate  $a + bk^2$ , with  $k^2 \ll 1$  and  $a/b > 1$ . Therefore the above considered triplet of graphs with zero, one, and two Debye lines, respectively, is asymptotically equivalent to

$$(a + bk^2)^{-1} \left( 1 - \frac{2}{k^2 + 1} + \frac{1}{(k^2 + 1)^2} \right) \approx \frac{2b}{a^2} \left( \frac{1 + b/a}{1 - b/a} \right) k^2, \quad k^2 \ll 1 \quad (5.2)$$

vanishing in the  $a/b \rightarrow \infty$  limit. The smaller estimate is obtained for the steeper asymptotic decrease, so that the most numerous compact structures eliminate themselves in the asymptotic range provided one considers not only a bridge graph alone but also its descendent within the same order. As expected the estimate (5.2) allows us to deduce  $\lim_{r \rightarrow \infty} w_2(r)$  from the much-less-numerous longest graphs within each order. Before leaving this section, it remains to comment a little bit more on the situation where the ascendent graph is not simple, and therefore missing in the nodal  $w_2(r)$  expansion. In this case, (5.2) has to be restricted to the last two terms on the left-hand side, which leaves unchanged the present statement because the corresponding  $a/b$  ratio is surely  $\gg 1$ . Another way to reach the same conclusion is to consider the  $g_2(r)$  nodal expansion itself where the nodal class is enlarged to include the  $w_2(r)$  12

reducible graphs,<sup>9</sup> so that the estimate (5.2) remains unchanged.

#### B. $\Lambda$ expansion of $\lim_{r \rightarrow \infty} w_2(r)$

Now, we are allowed to build a  $w_2(r)$   $\Lambda$  expansion in the asymptotic range from systematic resummations to infinity of the longest convolution chains.<sup>2,3,5</sup> First, let us consider with Mitchell and Ninham<sup>5</sup> the chains with  $c=n$  Debye lines and  $b=n-1$  two-bubbles ( $b+c=k+1$ ) in order to set up a simple example of the resummation procedure. So, we get the sum

$$\begin{aligned} \frac{2}{\pi r} \sum_{n=1}^{\infty} (-\Lambda)^n \int_0^{\infty} \frac{d\kappa \kappa \sin \kappa r}{(\kappa^2 + 1)^n} \left( \frac{\tan^{-1}(\kappa/2)}{2\kappa} \right)^{n-1} \\ = -\frac{2}{\pi r} \int_0^{\infty} \frac{d\kappa \kappa \sin \kappa r}{1 + \kappa^2 + (\Lambda/2\kappa) \tan^{-1}(\kappa/2)} \\ = -\frac{\Lambda e^{-(1+\Lambda/8+1/16)r}}{r} \end{aligned} \quad (5.3)$$

through a geometric series  $(n-1 \rightarrow n)$  summable as long as  $|\Lambda \tan^{-1}(\kappa/2)/2\kappa(\kappa^2 + 1)| < 1$ , i.e.,  $\Lambda < 4$ . Actually, we shall consider the left-hand side of Eq. (5.3) and its extensions considered below, for much larger  $\Lambda$  values, without paying further attention to the validity of such a procedure, which seems to work in such different areas of physics as equilibrium statistical mechanics and quantum electrodynamics<sup>17</sup> provided the resummation of a given class of terms is performed to infinity. Equation (5.3) is nothing but the sum of the longest convolution chains  $\sim (-\Lambda)^n r^{n-2} e^{-r}$  as  $r \rightarrow \infty$ . It displays a nearly Debye-like asymptotic decrease while each term exhibits a smoother decrease when  $n \rightarrow \infty$ . This feature illustrates the power of the previous treatment and allows us to trust the nodal expansion to every  $n$ .

A more complete result may be obtained by retaining all the leading chains with  $c=0, 1, \dots, n$ , with

$$w_2^2(r) = \sum_{n=2}^{\infty} \sum_{p=0}^n (-1)^p \binom{n}{p} \left( -\frac{\Lambda}{2} \right)^{n-1} \left( -\frac{2\Lambda}{\pi r} \right) \int_0^{\infty} \frac{d\kappa \kappa \sin \kappa r}{(\kappa^2 + 1)^{n-p}} \left( \frac{\tan^{-1}(\kappa/2)}{2\kappa} \right)^{n-1} - \frac{\Lambda^2}{\pi r} \int_0^{\infty} d\kappa \sin \kappa r \tan^{-1}(\kappa/2), \quad (5.4)$$

where the non-nodal<sup>12</sup> reducible two-bubbles have been subtracted out to secure the  $\kappa \rightarrow \infty$  summability. Performing first the binomial summation within each order yields

$$\frac{2\Lambda}{\pi r} \sum_{n=2}^{\infty} \left( \frac{\Lambda}{2} \right)^{n-1} \int_0^{\infty} d\kappa \kappa \sin \kappa r \left( \frac{\kappa^2}{\kappa^2 + 1} \right)^n \left( \frac{\tan^{-1}(\kappa/2)}{\kappa} \right)^{n-1} \quad (5.5)$$

for the first term on the right-hand side of Eq. (5.4), and summing up as before the geometric series

$$\begin{aligned} w_2^2(r) = r^{-1} \int_0^{\infty} d\kappa \kappa \sin \kappa r \left[ \frac{2\Lambda}{\pi} \sum_{n=0}^{\infty} \left( \frac{\Lambda}{2} \right)^{n+1} \left( \frac{\kappa^2}{\kappa^2 + 1} \right)^{n+2} \left( \frac{\tan^{-1}(\kappa/2)}{\kappa} \right)^{n+1} - \frac{\Lambda^2 \tan^{-1}(\kappa/2)}{2} \frac{1}{\kappa} \right] \\ = \frac{2\Lambda^2}{\pi r} \int_0^{\infty} d\kappa \kappa \sin \kappa r \left[ \frac{\kappa^2}{\kappa^2 + 1} \frac{\tan^{-1}(\kappa/2)}{2\kappa} \frac{1}{1 + 1/\kappa^2 - (\Lambda/2\kappa) \tan^{-1}(\kappa/2)} - \frac{\tan^{-1}(\kappa/2)}{2\kappa} \right] \end{aligned} \quad (5.6)$$

with

$$\left| \frac{\Lambda}{2} \frac{\kappa^2}{\kappa^2+1} \frac{\tan^{-1}(\kappa/2)}{2\kappa} \right| \leq 1 \quad \text{if } \Lambda \leq 6$$

makes appear the well-known resummation supporting the hypernetted-chain (HNC) approximation (1.5) with the bubble function  $G$  conveniently restricted to its first term  $\Lambda^2 \tan^{-1}(\kappa/2)/2\kappa$ . Adding the first-order Debye line allows us to write the last line in the compact form<sup>2</sup>

$$w_2^2(r) = \frac{2\Lambda}{\pi r} \int_0^\infty d\kappa \kappa \sin\kappa r \left[ -\frac{1}{\kappa^2} + \frac{[-1/\kappa^2 + \Lambda \tan^{-1}(\kappa/2)/2\kappa]^2}{1 + 1/\kappa^2 - (\Lambda/2\kappa) \tan^{-1}(\kappa/2)} \right]. \quad (5.7)$$

The main interest of the present derivation lies in the transparent way the second-order graphs are resummed to infinity, thus making obvious the extensions to higher orders required to improve Eq. (1.5). The next approximation is expected to arise from analogous chains with one two-bubble replaced by a third-order nonconvolution graph either 12 irreducible as (3a) from Fig. 1 or 12 reducible as those depicted in Fig. 2. We do not need to worry about the reductibility character of a given structure. The quantity of interest is the sum of all the  $n$ -order nonconvolution graphs (with their multiplicity if any), which has to be iterated from order  $n$  to infinity. However, when further short-range resummations are considered as below, it proves useful to keep the reductibility character which allows us to remove most of the 12 reducible graphs. At the moment, let us introduce  $\beta_n(\kappa)$ , the above-defined sum of bridge graphs. For  $n=3$ , we get

$$\begin{aligned} w_2^3(r) &= \frac{2}{\pi r} \sum_{n=3}^\infty (-\Lambda)^3 \sum_{p=0}^{n-1} (-1)^p \left(-\frac{\Lambda}{2}\right)^{n-3} \binom{n-1}{p} \int_0^\infty \frac{d\kappa \kappa \sin\kappa r \beta_3(\kappa)}{(\kappa^2+1)^{n-1-p}} \left(\frac{\tan^{-1}(\kappa/2)}{\kappa}\right)^{n-3} \\ &= \frac{2\Lambda^3}{\pi r} \sum_{n=3}^\infty \left(\frac{\Lambda}{2}\right)^{n-3} \int_0^\infty d\kappa \kappa \sin\kappa r \beta_3(\kappa) \left(\frac{\kappa^2}{\kappa^2+1}\right)^{n-1} \left(\frac{\tan^{-1}(\kappa/2)}{\kappa}\right)^{n-3} \\ &= \frac{2\Lambda^3}{\pi r} \int_0^\infty d\kappa \kappa \sin\kappa r \left[ \frac{\kappa^2}{\kappa^2+1} \beta_3(\kappa) \frac{1}{1 + 1/\kappa^2 - (\Lambda/2\kappa) \tan^{-1}(\kappa/2)} - [12 \text{ reducible part of } \beta_3(\kappa)] \right], \end{aligned} \quad (5.8)$$

where the subtracted reducible part has been written in the last line only to save space. The usual geometric series is recovered with  $n-3 \rightarrow n$  in the second line. The same process works for all  $n$  with

$$\begin{aligned} w_2^n(r) &= \frac{2}{\pi r} \int_0^\infty d\kappa \kappa \sin\kappa r \left[ \frac{\kappa^2}{\kappa^2+1} \frac{G(\kappa) + \sum_{n=3}^\infty \Lambda^n \beta_n'(\kappa)}{1 + 1/\kappa^2 - (\Lambda/2\kappa) \tan^{-1}(\kappa/2)} \right. \\ &\quad \left. - \left( G(\kappa) + \sum_{n=3}^\infty \Lambda^n [12 \text{ reducible part of } \beta_n(\kappa)] \right) \right] - \frac{\Lambda e^{-r}}{r}, \end{aligned} \quad (5.9)$$

where  $\beta_n'(\kappa) = \beta_n(\kappa) - (n\text{-bubble})$  and  $G(\kappa) = 2\pi^2 f(\kappa)$  denotes the  $n$ -bubble sum investigated in Sec. IV.

A remarkable feature of these long-range resummations is the systematic appearance of  $G(\mathbf{k})$  introduced previously<sup>2</sup> in the second-order sum (5.7) on heuristic arguments. The only bridge graphs to remove in order to secure the large- $k$  summability are the 12 reducible ones, in accord with their short-range behavior, while the 12 irreducible ones were also subtracted out in Ref. 2. The resummation procedure may be pursued further with the replacement of two two-bubbles within the longest convolution chains. Specializing first to third-order bridge graphs, we have

$$\begin{aligned} w_2^{33}(r) &= \frac{2}{\pi r} \sum_{n=5}^\infty (-\Lambda)^n \int_0^\infty d\kappa \kappa \sin\kappa r \beta_3(\kappa) \beta_3(\kappa) \left(\frac{-\kappa^2}{\kappa^2+1}\right)^{n-2} \frac{[\tan^{-1}(\kappa/2)]^{n-5}}{2\kappa} \\ &= \frac{2\Lambda^5}{\pi r} \int_0^\infty d\kappa \kappa \sin\kappa r \left(\frac{\kappa^2}{\kappa^2+1}\right)^2 \frac{\beta_3(\kappa) \beta_3(\kappa)}{1 + 1/\kappa^2 - (\Lambda/2\kappa) \tan^{-1}(\kappa/2)}, \end{aligned} \quad (5.10)$$

with no spurious 12 reducible product to remove. This last step is again extendable to all  $n$ , with a number  $p$  of two-bubbles replaced by  $n$ -order bridge graphs. Thus

$$w_2^{n \cdots n}(r) = \frac{2}{\pi r} \sum_{p=2}^\infty \int_0^\infty \left(\frac{\kappa^2}{\kappa^2+1}\right)^p \sum_{n_1, n_2, \dots, n_p=3}^\infty \Lambda^A \frac{\kappa \sin\kappa r \beta_{n_1}(\kappa) \cdots \beta_{n_p}(\kappa)}{1 + 1/\kappa^2 - (\Lambda/2\kappa) \tan^{-1}(\kappa/2)} d\kappa, \quad (5.11)$$

where the  $A$  in  $\Lambda^A$  is  $A = \sum_{i=1}^p n_i + 1 - p$ , represents the maximal extension of the iteration to infinity of the longest convolution chains built from every possible combination of nonconvolution graphs with two-bubbles and Debye lines. The  $n_i$  sum is restricted to count every  $\beta_{n_1}(\kappa) \cdots \beta_{n_p}(\kappa)$  product only once. Collecting altogether Eqs. (5.9) and (5.11), the complete asymptotic expansion of  $w_2(r)$  is written as

$$\begin{aligned} \lim_{r \rightarrow \infty} w_2(r) &= w_2^n(r) + w_2^{n \cdots n}(r) \\ &= -\frac{\Lambda e^{-r}}{r} + \frac{2}{\pi r} \int_0^\infty d\kappa \kappa \sin \kappa r \left\{ \frac{\kappa^2}{\kappa^2 + 1} \left[ G(\kappa) + \sum_{n=3}^\infty \Lambda^n \beta_n'(\kappa) + \sum_{p=2}^\infty \left( \frac{\kappa^2}{\kappa^2 + 1} \right)^{p-1} \sum_{n_1, n_2, \dots, n_p=3}^\infty \Lambda^A \beta_{n_1}(\kappa) \cdots \beta_{n_p}(\kappa) \right] \right. \\ &\quad \times \left[ 1 + \frac{1}{\kappa^2} - \frac{\Lambda}{2\kappa} \tan^{-1} \left( \frac{\kappa}{2} \right) \right]^{-1} - G(\kappa) \\ &\quad \left. - \sum_{n=3}^\infty \Lambda^n [12 \text{ reducible part of } \beta_n(\kappa)] \right\}, \end{aligned} \quad (5.12)$$

which is completely determined once we know the  $\beta_n(\kappa)$  asymptotic behavior. At first sight, it should be tempting to approximate  $\beta_3(\kappa)$  and  $\beta_4(\kappa)$  with their asymptotic estimates obtained in Sec. III. As an example, Eqs. (3.7) and (3.29) provide

$$\beta_3'(\kappa) = \frac{3\pi}{27 + 8\kappa^2} + \frac{7}{8} \left( \frac{\ln 3}{2 + \kappa^2/6} + \frac{2}{9 + \kappa^2/9} \right) + \frac{1}{4} \left( \frac{1}{9 + 19\kappa^2/12} + \frac{1}{3 + \kappa^2/9} \right), \quad \kappa^2 \ll 1. \quad (5.13)$$

However, it proves much more interesting to eliminate most of the 12 reducible graphs through further short-range resummations.  $\beta_n'(\kappa)$  and  $\beta_n(\kappa)$  are then restricted to their 12 irreducible parts. For instance

$$\beta_3'(\kappa) \rightarrow \frac{-3\pi}{27 + 8\kappa^2}.$$

These short-range resummations are easily monitored by the  $n$ -bubble sum  $G(\kappa)$ , as explained in Fig. 9 for the third-order 12 irreducible bridge graph, through iteration to infinity of the same topological structure ( $k$  fixed) with increasing multiplicity of a given bond. A first striking by-product of these simple manipulations is to enhance the relative asymptotic preeminence of the 12 irreducible graphs with single bonds only, in accordance with the faster-than-Debye decrease of the short-range resummation and the reduction of the order in  $\Lambda$  of the resummed multiple-bonded graphs. The last argument applies for  $\Lambda \geq 1$ . These remarks prove the above-mentioned negligibility of the  $\beta_n'(\kappa)$  and  $\beta_n(\kappa)$  reducible parts, while the subtracted sum in Eq. (5.12) starts from  $n = 4$

with the first 12 reducible single-bonded graph. So far, we have only taken into account the convolution chains built from  $n - 1$  two-bubbles or bridge graphs with  $l > 2(n - 1)$ . It then remains to pay attention to the faster decreasing chains with  $l < 2(n - 1)$ . They are of importance for an accurate determination of the  $r$  value where the  $g_2(r)$  short-range oscillations set in. The corresponding series do not exist within each order. For instance, the third-order compact graphs reappear every two orders only in longer chains with three-bubbles and Debye lines.

Schematically, a chain built from three-bubbles only cannot be resummed the way a two-bubble series is (geometric series). The corresponding series are lacunary and more involved than the previous ones. Nevertheless, an appropriate approximation may be obtained by retaining the  $n$ -bubbles ( $n \geq 3$ ) and the 12 irreducible bridge graphs in the way they appear in the numerator of Eq. (5.12), i.e., the dominant contributions in the small- $r$  limit, to every order, and replace one, two  $n$ -bubbles by a bridge graph as above. As a consequence the only change in Eq. (5.12) is the extension of the two-bubble  $(\Lambda/2\kappa) \tan^{-1}(\kappa/2)$  in the denominator to the sum  $G'(\kappa)/\Lambda$ , where

$$G'(\kappa) = G(\kappa) + \sum_{n=3}^\infty \Lambda^3 \beta_n^*(\kappa) + \sum_{p=2}^\infty \left( \frac{\kappa^2}{\kappa^2 + 1} \right)^{p-1} \sum_{n_1, n_2, \dots, n_p}^\infty \Lambda^A \beta_{n_1}^*(\kappa) \cdots \beta_{n_p}^*(\kappa), \quad (4.7')$$

thus making explicit, through the neglect of the  $\beta^*$ 's, the extrapolation used in Ref. 2. As a conclusion, the above discussion is summarized in the final asymptotic expression

$$\lim_{r \rightarrow \infty} w_2(r) = -\frac{\Lambda e^{-r}}{r} + \frac{2}{\pi r} \int_0^\infty dk \kappa \sin \kappa r \left\{ \frac{\kappa^2}{\kappa^2 + 1} \left[ G(\kappa) + \sum_{n=3}^\infty \Lambda^3 \beta_n^*(\kappa) + \sum_{p=2}^\infty \left( \frac{\kappa^2}{\kappa^2 + 1} \right)^{p-1} \sum_{n_1, n_2, \dots, n_p=3}^\infty \Lambda^4 \beta_{n_1}^*(\kappa) \cdots \beta_{n_p}^*(\kappa) \right] \right. \\ \left. \times \left[ 1 + \frac{1}{\kappa^2} - \frac{G'(\kappa)}{\Lambda} \right]^{-1} - G(\kappa) - \sum_{n=1}^\infty \Lambda^n \beta_n^*(\kappa) \right\}, \tag{5.14}$$

with  $\beta_n^*(\kappa)$  the 12 irreducible single-bonded part of  $\beta_n(\kappa)$  and  $\beta_n^\dagger(\kappa)$  the 12 reducible single-bonded part of  $\beta_n(\kappa)$ . The numerical results obtained in Sec. III allow a reasonable approximation of Eq. (5.14) with

$$\beta_3^*(\kappa) \sim - (0.34907 - 0.10343 \kappa^2) \text{ as } \kappa \rightarrow 0, \\ \beta_4^*(\kappa) \sim - (0.14912 - 0.04019 \kappa^2) \text{ as } \kappa \rightarrow 0, \tag{5.15} \\ \beta_4^\dagger(\kappa) \sim 2(0.13594 - 0.0089544 \kappa^2) \text{ as } \kappa \rightarrow 0,$$

and  $3 \leq n, n_1, n_2, \dots, n_p \leq 4$  for  $\Lambda \geq 1$ . It must be stressed out that the above  $\kappa$  quadrature should be

accurate for all  $\kappa$ . Then we need a good estimate for the bridge graphs even in the short-range limit  $\kappa \rightarrow \infty$ , which is outside the scope of the present work. This explains why we refrain from giving extensive numerical estimates for the  $n$  and  $p$  sums in Eq. (5.14). However, we have shown previously that the third-order 12 irreducible bridge graph is well approximated by its asymptotic value over a very large domain.

It allows for the first straightforward, although nontrivial, correction to the usual (second-order) HNC approximation<sup>2,6</sup>

$$\lim_{r \rightarrow \infty} w_2^3(r) = -\frac{\Lambda e^{-r}}{r} + \frac{2}{\pi r} \int_0^\infty dk k \sin kr \left( \frac{k^2}{k^2 + 1} \left[ G(k) - \frac{3\pi\Lambda^3}{27 + 8k^2} + \sum_{p=2}^\infty \left( \frac{k^2}{k^2 + 1} \right)^{p-1} \Lambda^{2p-1} \left( \frac{3\pi\Lambda^3}{27 + 8k^2} \right)^p \right] \right. \\ \left. \times \left\{ 1 + \frac{1}{k^2} - \left[ \frac{G(k)}{\Lambda} - \frac{3\pi\Lambda^2}{27 + 8k^2} + \sum_{p=2}^\infty \left( \frac{k^2}{k^2 + 1} \right)^{p-1} \Lambda^{2p-2} \left( \frac{3\pi\Lambda^3}{27 + 8k^2} \right)^p \right] \right\}^{-1} \right. \\ \left. - G(k) - \frac{2(0.13594)^2}{0.13594 + 0.008954 k^2} \right). \tag{5.16}$$

The fourth-order extension of Eq. (5.6) is obtained by replacing the third-order bracket with

$$\sum_{n=3}^4 \Lambda^n \beta_n^*(k) + \sum_{p=2}^\infty \left( \frac{k^2}{k^2 + 1} \right)^{p-1} \sum_{i=0}^p \beta_3^*(k)^{p-1} \beta_4^*(k)^i \Lambda^{2p+1+i}. \tag{5.17}$$

Finally, extrapolating the decreasing behavior  $\beta_n(k) \rightarrow 0$  as  $n \rightarrow \infty$ , for  $k^2 \ll 1$ , from the third- and fourth-order asymptotic calculations performed in Sec. III, one is tempted to conjecture that the complete expression (5.14) may be written in the general form

$$\lim_{r \rightarrow \infty} w_2(r) = -\frac{\Lambda e^{-r}}{r} + \frac{2}{\pi r} \int_0^\infty dk k \sin kr \left( \frac{[k^2/(k^2 + 1)]G_1(k)}{1 + 1/k^2 - G'(k)/\Lambda} - G_2(k) \right), \tag{5.18}$$

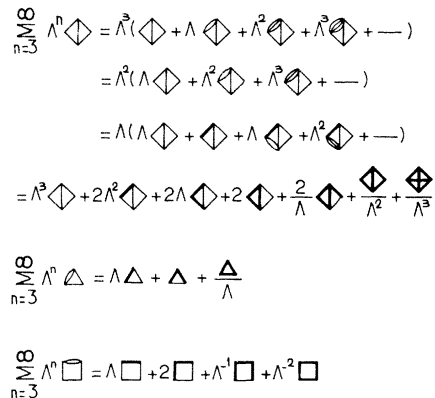


FIG. 9. Short-range resummation of third-order non-convolution graphs ( $\Lambda \geq 1$ ). An ordinary line represents a Debye line, while a heavy line represents an  $n$ -bubble sum.

with

$$G_2(k) \sim G_1(k) = G'(k). \quad (5.19)$$

The latter estimation constitutes the bulk of our statement. It seems to be supported by Eq. (5.1), where the  $p$  sum is alternating and decreasing with  $p \rightarrow \infty$  for fixed  $\Lambda$ . This plausibility argument could explain the success of the usual numerical procedure based on Eqs. (1.2)–(1.5), while it allows for a systematic improvement of  $G_2 - G'$ , with the aid of a complete calculation of the bridge graphs considered in a future work.

### C. Onset of short-range order

In their important work,<sup>2</sup> Del Rio and De Witt have shown that the onset of short-range order may be observed through the development of small-amplitude oscillations of  $g_2(r)$  around unity, arising from the coalescence on the positive imaginary  $k$  axis of the two roots of the equation

$$1 + \frac{1}{k^2} - \frac{G(k)}{\Lambda} = 0. \quad (5.20)$$

To solve this these authors have approximated (4.10) with its first term and have obtained a critical  $\Lambda$  value which is  $\Lambda_c = 4.225$ .

With a view towards elaborating their calculation, we first use the asymptotic expression (4.11) for  $G(k)$  which retains the corresponding  $n$ -bubble contribution to all  $n$  and neglect the bridge terms. The coalescence of the two roots occurs for  $[1 - \Lambda A(\Lambda)]^2 = 4\Lambda B(\Lambda)$  at  $\Lambda_c = 7.307$ , or  $\Gamma_c = e^2/k_B T a = 2.611$  with  $a = (4\pi m_i/3)^{-1/3}$ , to which corresponds the critical  $k$  value,  $k_c = 1.807i$ .

Although this result is apparently in good agreement with Hansen's recent Monte Carlo calculations,<sup>8</sup> the fact that  $|k_c| > 1$  invalidates our small- $k$  expansion of  $G(k)$ . To remedy this drawback, we then have been led to solve (5.20) with the full expression (4.9) for  $G(k)$ . The critical  $\Lambda$  value is found to be  $\Lambda_c = 4.247$  and  $k_c = iv_c = 1.498i$ .

This is in excellent agreement with Del Rio–De Witt's result.<sup>2</sup> Then the corresponding potential of average force  $w_2(r)$  can be obtained by the inverse Fourier transform

$$w_2(r) = -\frac{\Lambda_c}{r} + \frac{2\Lambda_c}{\pi r} \int_0^\infty dk k \operatorname{sinc} kr \frac{[-1/k^2 + G(k)/\Lambda_c]^2}{1 + 1/k^2 - G(k)/\Lambda_c}, \quad (5.21)$$

an expression equivalent to (5.18) when  $G_1(k) = G_2(k) = G(k)$ . Assuming that the integral exists, we obtain

$$w_2(r) = -(\Lambda_c/r) [\nu(3 - v_c r) e^{-v_c r}], \quad (5.22)$$

where

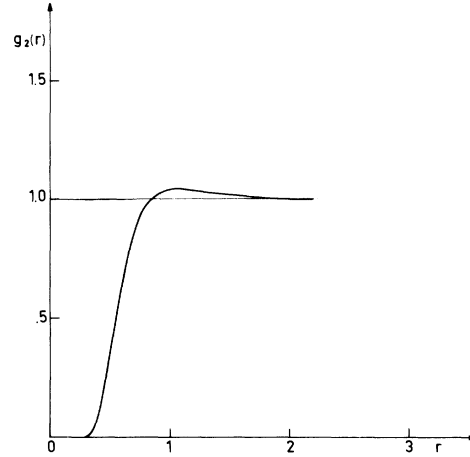


FIG. 10.  $g_2(r)$  at  $\Lambda = \Lambda_c = 4.247$ ;  $r$  in number of  $a = (\frac{4}{3}\pi n)^{-1/3}$ .

$$\nu = 2v_c^4 \left[ 1 + \frac{v_c^3}{2} \frac{d^2}{dk^2} \left( \frac{k}{\Lambda} G(k) \right) \right]_{k=iv_c}^{-1} = 1.374.$$

The behavior of  $g_2(r)$  ( $=e^{w_2(r)}$ ) at  $\Lambda_c$  is shown in Fig. 10. We observe in this figure no small-amplitude oscillation of  $g_2(r)$ , but only a damping. The onset of short-range order would take place when  $\Lambda > \Lambda_c$ . The discrepancies between this last  $\Lambda_c$  value and the Monte Carlo ones<sup>8</sup> may well be accounted for by our present neglect of the bridge graphs. Unfortunately, the required computations would need accurate  $\beta_n^*(k)$  for all  $k$ , which are very far from us at the moment. On the other hand, if  $G(k)$  is restricted to its first two-bubble term, Eq. (5.20) yields  $\Gamma_c \sim 1$ , in accord with a self-consistent approximation worked out by Choquard and Sari.<sup>18</sup> This last value means that the onset of short-range order would then be expected to take place when the mean kinetic energy approaches the mean interparticle potential energy. Indeed, without any explicit evaluations of the bridge contributions, it is not possible to guess the right  $\Lambda_c$  value among the above three proposals. Possibly, numerical inversion of Monte Carlo data performed by De Witt<sup>19</sup> would overcome that difficulty.

### ACKNOWLEDGMENTS

The motivation for this work was given to us in a discussion with H. E. De Witt and C. F. Hooper, Jr. Stimulating discussions with A. A. Broyles, J. Groeneveld, J. P. Hansen, B. Jancovici, M. Lavaud, D. Levesque, and M. A. Pokrant have also been useful. The hospitality extended to one of us (C.D.) by the Research Laboratory of Electronics of the Massachusetts Institute of Technology, where part of this work has been completed, is also gratefully acknowledged.

## APPENDIX A

Here we give the derivation of the Mitchell-Ninham relation (3.5) and its extensions. Let us start from the relations (the first is Goursat-Feynmann)

$$\frac{1}{ab} = \int_0^1 \frac{dx}{[ax + b(1-x)]^2}, \quad (\text{A1})$$

$$\int \frac{d\vec{Q}}{(Q^2 + a^2)[(\vec{Q} + \vec{k})^2 + B^2]^2} = \frac{2\pi^2}{B} \frac{1}{[k^2 + (a+B)^2]}, \quad (\text{A2})$$

which give

$$\begin{aligned} I_2 &= \int \frac{d\vec{Q}}{(Q^2 + a^2)[(\vec{Q} + \vec{k})^2 + B^2][(\vec{Q} + \vec{P}_1)^2 + \gamma^2][(\vec{Q} + \vec{P}_2)^2 + \sigma^2]} \\ &= \int_0^1 dx \int \frac{d\vec{Q}}{[(\vec{Q} + \vec{P}_1)^2 + \gamma^2][(\vec{Q} + \vec{P}_2)^2 + \sigma^2][(\vec{Q} + x\vec{k})^2 + \delta^2]^2} \\ &= \int_0^1 dx \int \frac{d\vec{Q}}{(Q^2 + a^2)[(\vec{Q} + \vec{P}_2 - \vec{P}_1)^2 + \sigma^2][(\vec{Q} + x\vec{k} - \vec{P}_1)^2 + \delta^2]^2}. \end{aligned} \quad (\text{A4})$$

The last line is obtained with  $\vec{Q} + \vec{P}_1 - \vec{Q}$ . The differentiation of Eq. (A3) with respect to  $\gamma$  yields

$$\begin{aligned} \int \frac{d\vec{Q}}{(Q^2 + a^2)[(\vec{Q} + \vec{k})^2 + \beta^2][(\vec{Q} + \vec{P})^2 + \gamma^2]^2} \\ = \frac{\pi^2}{\gamma} \int_0^1 \frac{dx}{\delta} \frac{\gamma + \delta}{[(\vec{P} - x\vec{k})^2 + (\gamma + \delta)^2]}. \end{aligned} \quad (\text{A5})$$

Setting now  $\alpha = \gamma$ ,  $\vec{k} = \vec{P}_2 - \vec{P}_1$ ,  $\beta = \sigma$ ,  $\vec{P} = x\vec{k} - \vec{P}_1$ , and  $\gamma = \delta$ , we obtain

$$\begin{aligned} I_2 &= \pi^2 \int_0^1 \frac{dx}{\delta} \\ &\quad \times \int_0^1 \frac{dy}{\delta'} \frac{\delta + \delta'}{[x\vec{k} - \vec{P}_1 - y(\vec{P}_2 - \vec{P}_1)]^2 + (\delta + \delta')^2]^2}, \end{aligned} \quad (\text{A6})$$

with  $\delta'^2 = y(1-y)(\vec{P}_2 - \vec{P}_1)^2 + \sigma^2 y + \gamma^2(1-y)$ . Identical methods may be used for

$$I_n \equiv \int d\vec{Q} \frac{1}{(Q^2 + a^2)[(\vec{Q} + \vec{k})^2 + \beta^2] \prod_{\gamma=1}^n [(\vec{Q} + \vec{P}_\gamma)^2 + \gamma^2]}. \quad (\text{A7})$$

## APPENDIX B

We intend to demonstrate that the pinched compact subgraphs appearing on the right-hand side of Eq. (4.2) decrease as  $r^m e^{-2r}$  or faster, in the asymptotic range. First, let us pay attention to the subgraphs depicted in Fig. 4, which are the compact graphs with the smallest line connection degree

$$\begin{aligned} I_1 &= \int \frac{d\vec{Q}}{(Q^2 + a^2)[(\vec{Q} + \vec{k})^2 + B^2][(\vec{Q} + \vec{P})^2 + \gamma^2]} \\ &= \int_0^1 dx \int \frac{d\vec{Q}}{[(\vec{Q} + \vec{P})^2 + \gamma^2][(\vec{Q} + x\vec{k})^2 + \delta^2]^2} \\ &= \pi^2 \int_0^1 \frac{dx}{\delta[(\vec{P} - x\vec{k})^2 + (\gamma + \delta)^2]}, \end{aligned} \quad (\text{A3})$$

where  $\delta^2 = x(1-x)k^2 + xB^2 + (1-x)a^2$ , i.e., the required result (3.5). Further extensions to the fourth-order bridge graphs necessitate the evaluation of the integral

$I' = 2$ , and restrict ourselves to the simplest third-order graph in this series. The corresponding pinched graph is the convolution product of two two-bubbles, which we now consider. It reads (with obvious notations)

$$\begin{aligned} g_3^{2,2}(r) &= \frac{(4\pi)^2}{2\pi^2 r} \int_0^\infty dk k \sin kr \left( \frac{\tan^{-1}(k/2)}{2k} \right)^2 \\ &= \frac{2}{r} \int_0^\infty dx \frac{e^{-2x}}{x} \int_0^\infty dy \frac{e^{-2y}}{y} \\ &\quad \times \int_0^\infty \frac{dk}{k} \sin kr \sin kx \sin ky \\ &= \frac{1}{r} \int_0^\infty \frac{dx}{x} e^{-2x} \int_0^\infty \frac{dy}{y} e^{-2y} \\ &\quad \times \int_0^\infty \frac{dk}{k} \sin kx [\cos k(r-y) \\ &\quad \quad \quad - \cos k(r+y)], \end{aligned} \quad (\text{B1})$$

obtained through the substitution

$$\tan^{-1}\left(\frac{k}{B}\right) = \int_0^\infty dx e^{-Bx} \frac{\sin kx}{x}. \quad (\text{B2})$$

The relationship

$$\int_0^\infty dx \frac{\sin ax \cos bx}{x} = \begin{cases} \pi/2, & a > b \geq 0 \\ \pi/4, & b = a > 0 \\ 0, & b > a \geq 0 \end{cases} \quad (\text{B3})$$

makes appear

$$\begin{aligned}
g_3^{2,2}(r) &= \frac{1}{2r} \int_0^\infty dx \frac{e^{-2x}}{x} [\text{Ei}(-2x - 2r) - \text{Ei}(-2|r - x|)] \\
&= \frac{1}{2r} \int_{-\infty}^\infty dx \frac{e^{-|x-2r|}}{|x-2r|} \text{Ei}(-|x|) \\
&= \frac{1}{2r} \left[ \int_1^\infty dt \ln t \frac{d}{dt} [e^{2rt} \text{Ei}(-2r(1+t)) - e^{-2rt} \text{Ei}(2r(t-1)) + e^{-2r} \text{Ei}(-2r(t-1)) - e^{2r} \text{Ei}(-2r(t+1))] \right] \\
&= -\frac{e^{-2r}}{2r} \left( \int_2^\infty \frac{dt}{t-1} [e^{2rt} \text{Ei}(-2rt) - e^{2r} \text{Ei}(-2rt)] + \int_0^\infty \frac{dt}{t+1} [e^{-2rt} \text{Ei}(2rt) + \text{Ei}(-2rt)] \right). \quad (\text{B4})
\end{aligned}$$

The last line is obtained with the aid of

$$\text{Ei}(-x) = -x \int_0^\infty dt \ln t e^{-tx}. \quad (\text{B5})$$

Equation (B4) may then be given the compact form

$$g_3^{2,2}(r) = \frac{e^{-2r}}{r} \text{P} \int_{-\infty}^\infty dt \frac{\text{Ei}(-2r|t|) f(t)}{t-1}, \quad (\text{B6})$$

with

$$f(t) = \begin{cases} 1, & t < 0 \\ e^{2rt}, & 0 < t < 2 \\ e^{4r}, & t > 2 \end{cases} \quad (\text{B7})$$

and

$$\int_0^\infty \left( \frac{e^{-ax} \text{Ei}(ax)}{x-b} - \frac{e^{ax} \text{Ei}(-ax)}{x+b} \right) dx = \begin{cases} 0, & ab < 0 \\ \pi^2 e^{-ab}, & ab > 0 \end{cases}.$$

Thus we get the asymptotic estimate<sup>20</sup>

$$\begin{aligned}
g_3^{3,0}(k) &= \frac{4\pi}{6(1 - 4/c^2 \lambda_D^2)^{3/2} k} \int_0^\infty dk k \sin kr \left( \frac{e^{-\alpha_1 r} - e^{-\alpha_2 r}}{r} \right)^3 \\
&= \frac{4\pi}{6(1 - 4/c^2 \lambda_D^2)^{3/2} k} \left\{ \left[ 3\alpha_1 \tan^{-1} \left( \frac{k}{3\alpha_1} \right) - 3(2\alpha_1 + \alpha_2) \tan^{-1} \left( \frac{k}{2\alpha_1 + \alpha_2} \right) + 3(\alpha_1 + 2\alpha_2) \tan^{-1} \left( \frac{k}{\alpha_1 + 2\alpha_2} \right) \right. \right. \\
&\quad \left. \left. - 3\alpha_2 \tan^{-1} \left( \frac{k}{3\alpha_2} \right) \right] + \frac{k}{2} \left\{ \ln(k^2 + 9\alpha_1^2) - 3 \ln[k^2 + (2\alpha_1 + \alpha_2)^2] \right. \right. \\
&\quad \left. \left. + 3 \ln[k^2 + (\alpha_1 + 2\alpha_2)^2] - \ln(k^2 + 9\alpha_2^2) \right\} \right\} \quad (\text{B10})
\end{aligned}$$

is considered in the classical limit<sup>11</sup> ( $\alpha_2 \gg \alpha_1 \sim 1$ ) with the diffraction corrections taken as a kind of Tauberian parameter. In the asymptotic domain, Eq. (B10) reduces to

$$g_3^{3,0}(k) \sim \frac{4\pi}{k} \tan^{-1} \left( \frac{k}{3} \right), \quad k \rightarrow 0. \quad (\text{B11})$$

Then results may be extended to a  $p$ -bubble with<sup>11</sup>

$$g_3^{p,0}(k) \sim \frac{4\pi}{k} \tan^{-1} \left( \frac{k}{p} \right), \quad k \rightarrow 0. \quad (\text{B12})$$

Therefore, the asymptotic estimates of convolution products of two-bubbles and three-bubbles, etc., may be worked out as above. For instance, we obtain

$$g_3^{2,2}(r) \sim \frac{e^{2r}}{4r^2} \int_2^\infty \frac{dt e^{-2rt}}{t(t-1)} \simeq \frac{e^{-2r}}{4r^3}, \quad \text{as } r \rightarrow \infty, \quad (\text{B8})$$

thus making clear that the given convolution product does not decay slower than the basic two-bubble, a behavior contrasting with that of the convolution chains ( $I' = 1$ ), i.e., containing Debye lines. Indeed in the latter situation, the asymptotic decrease is monitored by the  $k = i$  pole, which is not the case presently. The asymptotic equivalent (B8) allows us to replace in a chain (of Fig. 5) a convolution product of two two-bubbles with one two-bubble in the asymptotic range. Going further in the same way, one obtains<sup>20</sup>

$$g_n^{2,2,\dots,2}(r) < e^{-2r/r^2}, \quad r \rightarrow \infty \quad (\text{B9})$$

for all  $n \geq 3$ , and for  $p$  2's. The same procedure may be extended to a chain with three-bubbles, if the modified Debye interaction (1.6) is used as a kind of Tauberian trick to separate the diverging short-range  $r^{-3}$  behavior from its asymptotic behavior  $e^{-3r/r^3}$ . More precisely, the corresponding Fourier transform<sup>11</sup>

$$\begin{aligned}
g_3^{3,2}(r) &= \frac{2}{r} \int_0^\infty dx \frac{e^{-3x}}{x} \int_0^\infty dy \frac{e^{-2y}}{y} \\
&\quad \times \int_0^\infty \frac{dk}{k} \operatorname{sink} r \operatorname{sink} x \operatorname{sink} y \\
&= \frac{1}{r} \int_0^\infty dx \frac{e^{-13x-3r1}}{x-r} \operatorname{Ei}(-2|x|) \\
&= \frac{e^{-3r}}{2r} \left( - \int_{5/3}^\infty \frac{dt}{t-1} [e^{3rt} \operatorname{Ei}(-3rt) - e^{6r} \operatorname{Ei}(-3rt)] \right. \\
&\quad \left. - \int_{-1/3}^\infty \frac{dt}{t+1} [-e^{-3rt} \operatorname{Ei}(3rt) + \operatorname{Ei}(-3rt)] \right),
\end{aligned} \tag{B13}$$

with the corresponding asymptotic estimate ( $r \rightarrow \infty$ )

$$\begin{aligned}
G_3^{3,2}(r) &\sim \frac{e^{3r}}{2r} \int_{5/3}^\infty \frac{dt}{t-1} \operatorname{Ei}(-3rt) \simeq - \frac{e^{3r}}{6r^2} \int_{5/3}^\infty \frac{dt}{t-1} \frac{e^{-3rt}}{t} \\
&= - \frac{e^{3r}}{6r^2} \left( \int_{2/3}^\infty dt \frac{e^{-3r(t+1)}}{t} - \int_{5/3}^\infty \frac{dt}{t} e^{-3rt} \right) \\
&= - \frac{e^{3r}}{4r^2} [-\operatorname{Ei}(-2r) e^{-3r} + \operatorname{Ei}(-5r)] \simeq - \frac{3e^{-2r}}{40r^3}
\end{aligned} \tag{B14}$$

As previously, this asymptotic equivalent may be transferred to a chain with an arbitrary number of two-bubbles and three-bubbles. The same arguments apply to a chain built from three-bubbles, so that

$$g_n^{3,3,\dots,3}(r) < e^{-3r}/r^3, \quad r \rightarrow \infty, \quad n > 3. \tag{B15}$$

Finally, the faster-than- $e^{-2r}/r^2$  decrease may be transferred to any convolution product of  $p_i$ -bubbles

with  $p_i > 2$ .

So it remains to us to pay due attention to mixed convolution products of  $p$ -bubbles with genuine bridge graphs decaying as  $e^{-\alpha r}/r$  with  $\alpha > 1$ . The asymptotic estimates obtained above for the  $p$ -bubbles allow us to consider at once the convolution product of  $n$  bridge graphs with  $m$   $p$ -bubbles in the form

$$\begin{aligned}
&\frac{1}{r} \int_0^\infty \frac{dk k \operatorname{sink} r}{(k^2 + \alpha^2)^n} \left( \frac{\tan^{-1} k/p}{pk} \right)^m \\
&= \frac{i\pi}{r} \frac{d^{n-1}}{dk^{n-1}} \left[ \frac{ke^{ikr}}{(k+i\alpha)^n} \left( \frac{\tan^{-1}(k/p)}{pk} \right)^n \right]_{k=i\alpha} \\
&\sim r^{n-2} e^{-\alpha r} \quad \text{as } r \rightarrow \infty.
\end{aligned} \tag{B16}$$

The explicit calculations performed in Sec. III give us  $1 < \alpha < 2.5$ . However, these results could only be trusted to establish the crucial  $\alpha > 1$  behavior. The real  $\alpha$  values for a given bridge graph may be obtained in the following way: First, let us start from the estimate  $e^{-2r}/r^3$  obtained for the first third-order bridge graph. Then, working again the asymptotic behavior of the fourth-order bridge graphs along the scheme displayed by Eqs. (4.1)–(4.5) and using the above estimates, we see immediately that  $\alpha \geq 2$  to any  $n \geq 5$ . Therefore, we may state that any bridge graph decays at least as  $r^m e^{-2r}$  for  $r \rightarrow \infty$ . More generally, Eqs. (4.1)–(4.5) show that  $\alpha = I' = I$ . Thus, we have completed the proof that the compact graphs introduced in Eq. (4.2) are asymptotically equivalent to  $r^m e^{-I' r}$ .

<sup>1</sup>G. F. Chapline, H. E. DeWitt, and C. F. Hooper, Jr., UCRL report UCRL-76272, 1975 (unpublished).

<sup>2</sup>F. Del Rio and H. E. DeWitt, Phys. Fluids **12**, 791 (1969).

<sup>3</sup>E. G. D. Cohen and T. J. Murphy, Phys. Fluids **12**, 1404 (1969).

<sup>4</sup>C. Deutsch and M. Lavaud, Phys. Rev. Lett. **31**, 921 (1973).

<sup>5</sup>D. J. Mitchell and B. W. Ninham, Phys. Rev. **174**, 280 (1968).

<sup>6</sup>(a) M. S. Cooper, Phys. Rev. A **7**, 1 (1973); (b) J. F. Springer, M. A. Pokrant, and F. A. Stevens, Jr., J. Chem. Phys. **58**, 4863 (1973); (c) K. C. Ng, Ph.D. thesis, (University of Florida, Gainesville, 1974) (unpublished); J. Chem. Phys. **61**, 2680 (1974).

<sup>7</sup>S. G. Brush, H. L. Sahlín, and E. Teller, J. Chem. Phys. **45**, 2102 (1966).

<sup>8</sup>J. P. Hansen, Phys. Rev. A **8**, 3096 (1973).

<sup>9</sup>E. E. Salpeter, Ann. Phys. (N.Y.) **5**, 183 (1958).

<sup>10</sup>For a more formal discussion of this point, see J. M. J. van Leeuwen, J. Groeneveld, and J. De Boer, Physica (Utr.) **25**, 792 (1959).

<sup>11</sup>M. M. Gombert and C. Deutsch, Phys. Lett. **47A**, 473 (1974); C. Deutsch and M. M. Gombert, J. Math. Phys. **17**, 1077 (1976); S. G. Brush, H. E. DeWitt, and J. G.

Trulio, Nucl. Fusion **3**, 5 (1963).

<sup>12</sup>M. Lavaud (unpublished).

<sup>13</sup>An explicit calculation yields  $0.07463k^4 - 0.01801k^6 + 0.00428k^8$ , which supports the required conjecture.

<sup>14</sup>R. J. Riddell, Jr., and G. D. Uhlenbeck, J. Chem. Phys. **21**, 2056 (1953).

<sup>15</sup>The degree of connection is defined as the minimum number of nodal points to remove in order to make a given connected graph disconnected with respect to the root points.

<sup>16</sup>Further details will be given by Y. Furutani and C. Deutsch (unpublished).

<sup>17</sup>R. Omnes (private communication).

<sup>18</sup>Ph. Choquard and R. P. Sari, Phys. Lett. **A40**, 109 (1972).

<sup>19</sup>H. E. DeWitt (private communication).

<sup>20</sup>An independent complex analysis obtained in Ref. 12 provides the more accurate estimates

$$g_3^{3,2}(r) \simeq \frac{e^{-2r}}{r^2} \ln r \quad \text{and} \quad g_n^{2,2,\dots,2}(r) \simeq \frac{e^{-2r}}{r^2} (\ln r)^{p-1},$$

for  $p \geq 2$ 's, as  $r \rightarrow \infty$ . These new results induce only minor quantitative changes in our analysis.

<sup>21</sup>More generally, we consider products with an arbitrary number of convolution chains.